A Study on the Flow Characteristics with the Width of Annular Slit in Spiral Flow Nozzle

T. H. Kim †, T. Setoguchi* and Y. W. Lee**

Abstract

In comparison with previous researches for swirling flow, the spiral flow self-generated in the spiral flow nozzle has some different characteristics. It is not needed a compulsive tangential momentum to get its velocity component and has long potential core, relatively low swirl ratio, and high focusing ability. In this study, the self-generated mechanism of the spiral flow was clarified and the effect on the width of annular slit on spiral flow characteristics was investigated experimentally and numerically. As a result, the existence of tangential velocity component regardless of a compulsive angular momentum is clarified and the results obtained by experiment have a satisfactory agreement with those by numerical method, quantitatively and qualitatively.

Key Words : Boundary layer, Buffer, Coanda effect, recirculation, Etc.

1. Introduction

In general, the swirling flow needs a compulsive force to get tangential momentum in the nozzle. It means that a swirling flow nozzle has a complex structure and difficulty in manufacturing and maintenance, relatively. According to Horii et al., a unique nozzle called as spiral flow nozzle is not needed any extra device such as twisted tape inducer[6], swirler or swirl vane to generate it. In that, the spiral flow nozzle has some merits.

Furthermore, Horii[3][9] in his study reported that the spiral jet in the spiral flow nozzle is tightly formed and stable in comparison with normal turbulent jet by the flow visualization with laser. Nishizawa[11] investigated that the axial velocity distributions of the spiral flow in a straight pipe is almost equal to that in normal jet under same conditions and its rotating direction has clockwise or counter-clockwise irregularly with time. As presented in these previous researches, the spiral flow in the spiral flow nozzle has also some distinct flow characteristics in comparison with a conventional swirling jet and normal jets.

† Dept. of Mech. Eng., Pukyong Nat'l Univ.
E-mail: ares8730@daum.net
* Dept. of Mech. Eng., Saga Univ., Japan
** Dept. of Mech. Eng., Pukyong Nat'l Univ.

In recent years, due to its flow features mentioned above, it is applied to various industrial fields s uch as soil and granule transportation[7][12], dispe rsion and encapsulation of sub-micron powders [2], cutting of soft materials[10], optical fiber passi ng[4], concentration of a plasma energy flow[5] a nd so on.

However, the precise mechanism which without a forced tangential momentum, the spiral flow self-generated in spiral flow nozzle remains an unsolved problem yet regardless of many previous researches and applications.

The objectives of the present study are to clarify its generating mechanism and to investigate the flow characteristics for the change of nozzle geometry under a fixed pressure ratio of pressurized air in the buffer to the atmosphere around the nozzle, experimentally and numerically.

2. Experimental Apparatus

Fig. 1(a) and 1(b) show the schematic diagram of the experimental apparatus and detailed nozzle configuration, respectively. This apparatus is consi sted of air reservoir (2 m^3), valve, circular duct and test section (spiral flow nozzle). As shown in the lower part of this figure, four tubes from the end of the circular duct are connected with four inlets of the reservoir upstream of the annular slit. The

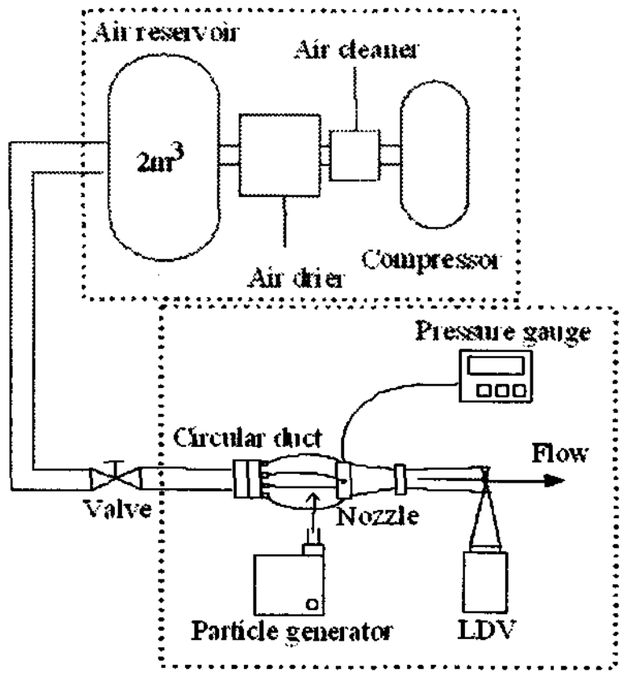

(a) Schematic diagram

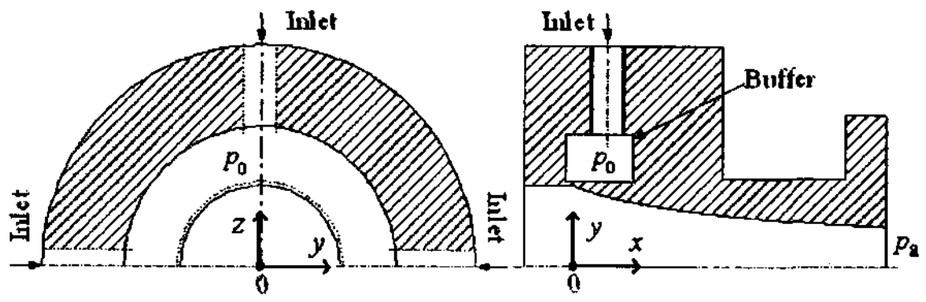

(b) Detailed nozzle configuration

Fig.1. Experimental apparatus

geometry of the spiral flow nozzle is almost the same as that used in the simulation. The ratio of the stagnation pressures p_o to p_a is 1.28 (p_o = 130.0 kPa and to p_a = 101.325 kPa).

The velocity distributions were measured downstream of the nozzle exit. A fiber-optic LDV system was used for velocity surveys. It consists of an argon-ion laser, a multicolor beam separator, a two-component fiber-optic probe system, signal processor, a 3-D traverse table driven by interface, and a personal computer with the flow information software. Laser probe was put on the 3-D traverse table that had a least step distance of 0.1 mm in each direction. The axial and tangential velocity components were measured at interval of 1.0 mm in the radial direction.

For every measurement point, 8000 data were sampled at least. All basic flow statistics could be drawn out with the processing of those data. As the acquisition mode used here was coincidence mode, the velocity components were obtained simultaneously and were statistically correlated.

This ensures that the velocities were measured from the same particle. Therefore, this acquisition is essential and accurately to measure the high velocity gradients inside the spiral flows.

The flow field was seeded with vapor by a particle generator that generated seeding particles with a diameter of 1 to 10 μm. This particle size is small enough to minimize errors in velocity measurements resulting from acceleration effects on the seed particles [1]. The Doppler-frequency of each channel was transformed into two velocity components through two real-time signal analyzers (RSA).

3. Numerical Method

In the present simulations, UPACS (Unified Platform for Aerospace Computational Simulation) [13] was used to investigate the spiral flow generated through an annular slit. This CFD code is the parallel CFD platform for multi-block grids which NAL (National Aerospace Laboratory: NAL was merged into the Japan Aerospace Exploration Agency (JAXA) with ISAS and NASDA of Japan on October 1st, in 2003) is developing for the purpose of the efficient CFD programming.

The parallel computational system was composed of five computers (Pentium 4 processor, 3.0 GHz) connected by a gigabit network. A message Passing Interface (MPI) was used for implementing parallel processing.

The governing equations under consideration are the unsteady compressible Navier -Stokes. A second-order finite volume scheme with MUSCL (Roe scheme) is used to discrete the spatial derivatives, and a second order-central difference scheme for the viscous terms, and a MFGS (Matrix Free Gauss Seidel) is employed for time integration. The Spalart-Allmaras model [8] was used as a turbulent model. The computational grids used in this simulation are shown in Fig. 2. The grid system in the computational domain is selected after the detailed grid refinement exercises and total grids used are approximately 1,200,000.

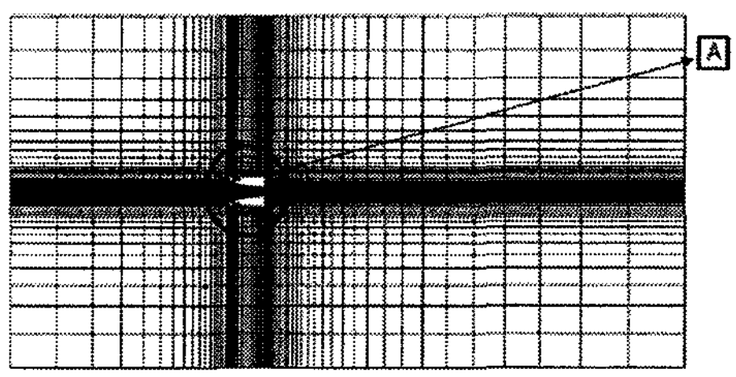

Fig.2. Computational Grids

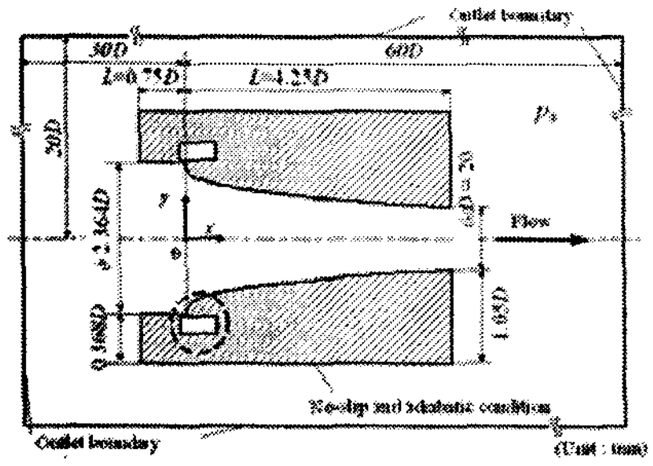

(a) Boundary conditions

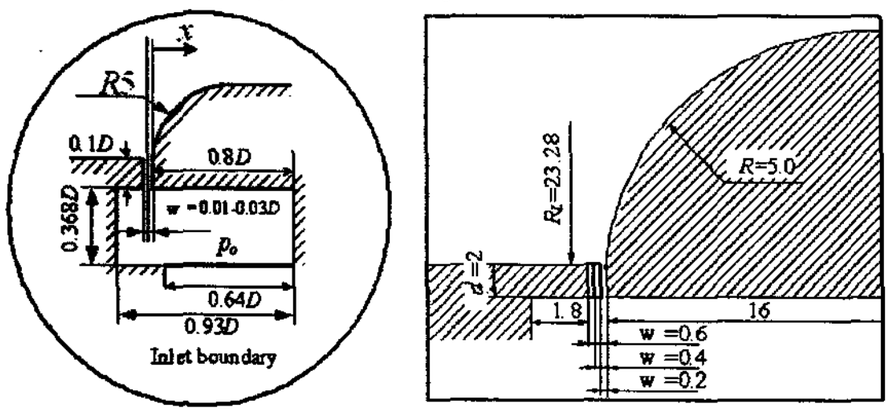

(b) Nozzle configurations

Fig.3. Boundary conditions and nozzle configuration

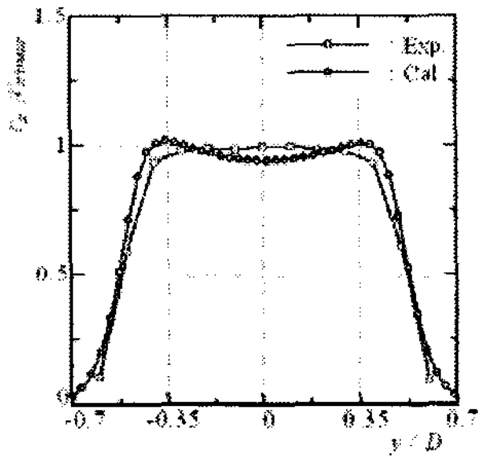

(a) Axial velocity distributions

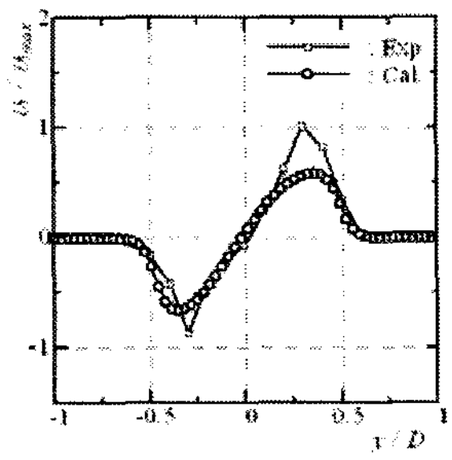

(b) Tangential velocity distributions

Fig.4. Velocity distributions in radial direction ($p_o / p_a = 1.28$, w = 0.6mm, $x / D = 4.75$)

Fig. 3 shows the details of a spiral flow nozzle and boundary conditions. The spiral nozzle has a circular cross section with a length L of 100 mm. The diameters at the exit and inlet of nozzle is 20 mm (= D) and 47.28 mm (= 2.364D), respectively. The radius of circular arc R for Coanda surface and height of the annular slit are 5.0 mm and 2 mm (= 0.1D), respectively. The beginning position of the Coanda surface coincides with the position of the exit of the slit. The x denotes the distance measured from Coanda surface side of the exit of the slit. The stagnation pressure p_a and temperature is 101.3 kPa and 298 K, respectively. The ratio of air pressure p_o in the buffer to atmospheric pressure p_a is constant, p_o / p_a = 1.28. However the width of the slit is changed from w = 0.6 mm to 0.2 mm. The wall boundary is set as adiabatic and no-slip condition. In the outflow, pressure is specified at the outlet boundary. The computational conditions used in the simulation are shown in Table 1.

Table 1 Computational conditions

Pressure ratio	Slit width (mm)
p_o / p_a = 1.28	0.2
	0.4
	0.6

4. Results and Discussion

Fig. 4 shows a comparison between the experimental and calculated results for axial and tangential velocity distributions in radial direction at the distance of x / D = 4.75 (at the distance of x / D = 0.5 from nozzle exit) after the time proceeds enough. The abscissa is the radial distance y measured from the nozzle centerline divided by the diameter of the nozzle exit D, and the ordinate is non-dimensionalized to the maximum of axial and tangential velocity obtained by the experiment. This comparison between experimental and calculated results for velocity distributions as shown in Fig. 4 shows a satisfactory agreement, quantitatively and qualitatively. However, the axial velocity distribution around the axis is relatively lagged in comparison with the experimental result. It is since the recirculation region in the nozzle inlet by the growth of boundary layer is relatively over-expected in the computation. Fig.5 shows the variation of pressure contours obtained in the cross-section of the buffer with the time. The compressible air supplied in the buffer through four rubber tubes from reservoir tank collides with the bottom of the buffer and it propagates to entire buffer region. Then, propagated air is stagnant in the position between ports and the pressure in this position goes up gradually. At initial time, the pressure contour in the buffer has axi-symmetric feature and then it change into asymmetric one. It means that the flow state in the buffer with time is very strongly unsteady and unstable. It is strongly

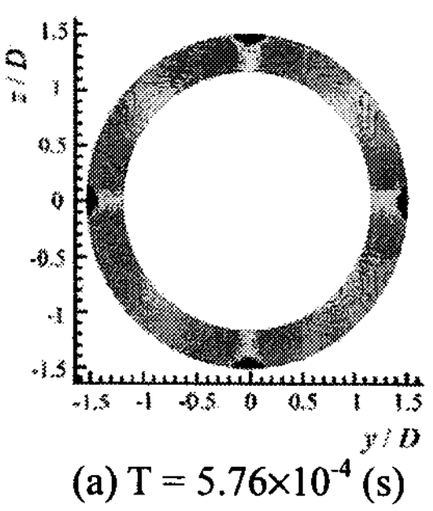

(a) $T = 5.76\times10^{-4}$ (s)

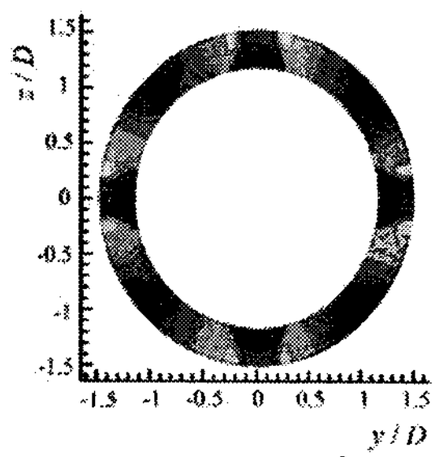

(b) $T = 2.78\times10^{-3}$ (s)

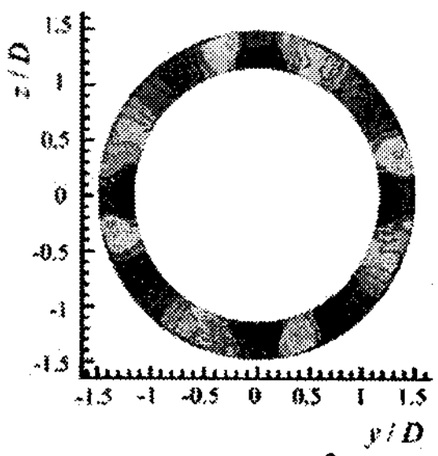

(c) $T = 2.3\times10^{-2}$ (s)

Fig. 5 The variation of pressure contours in the buffer with time ($p_o / p_a = 1.28$, w = 0.6 mm)

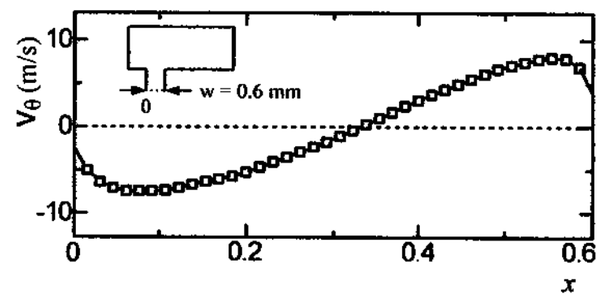

(a) Slit width = 0.6mm

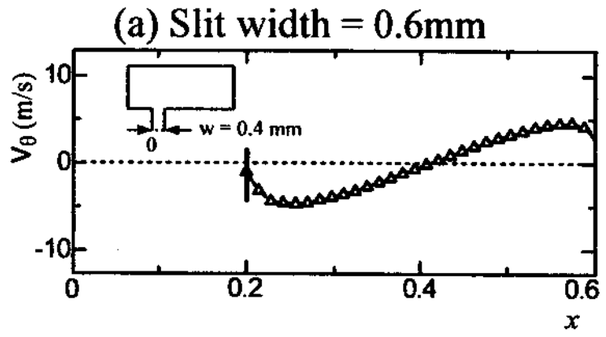

(b) Slit width = 0.4mm

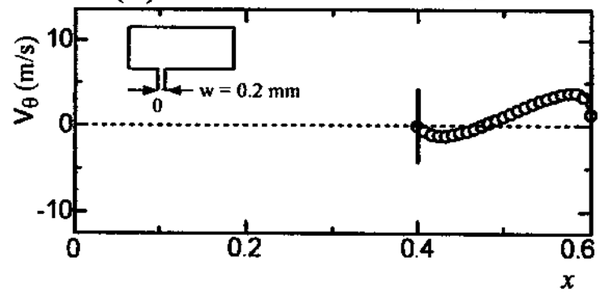

(c) Slit width = 0.2mm

Fig.6 Tangential velocity distributions at the tip of annular slit

related with the flow passing through annular slit. In other words, in the flow exhausted from annular slit, though normal velocity component to annular slit is dominant, the existence of other velocity components can be expected.

As expected, the existence of tangential velocity distributions at the tip of annular slit is clearly clarified in Fig. 6. It can be thought as the onset of spiral flow in the spiral flow nozzle. Under the same condition of pressure ratio, the magnitude of tangential velocity distribution detected at the tip of annular slit increases relatively as the slit width is getting wider. This result is depending on the compressible effect of air supplied from reservoir tank in the buffer. In other words, the decrease of slit width under the same condition denotes that the air in the buffer has stronger compressibility. As a result, the pressure gradient through the buffer of smaller slit is lower than other one and the flow state is relatively stable.

Fig. 7 indicates the flow process by tracking of streamlines in the nozzle. In the primary flow to have high momentum by passing through narrow slit, normal velocity component is dominant around the tip of annular slit. But, normal velocity is changed into axial velocity by the curvature surface connected with the tip of annular slit. The axial velocity has the transitional process in its velocity; acceleration, deceleration, and acceleration, by nozzle configuration. In addition, the difference of pressure between near annular slit and nozzle inlet generates the secondary flow from nozzle inlet. This primary flow and secondary flow forms the boundary layer in a vicinity of annular slit. This boundary layer develops to the nozzle downstream. By the developed boundary layer, a stagnant region in the nozzle is formed and the secondary flow induced from nozzle inlet is reversed by this boundary layer. As a result, the region of the flow recirculation is generated. It can be presumed that

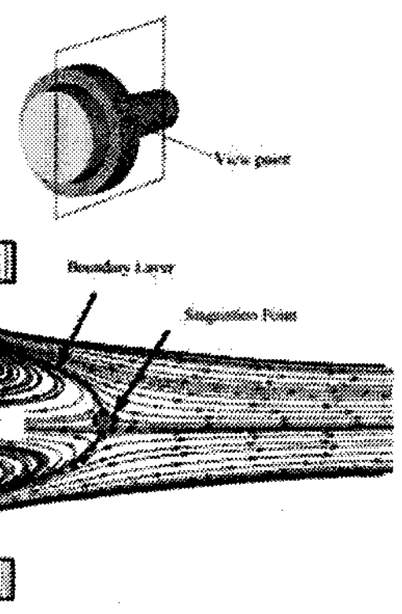

Fig.7. Flow process in the nozzle

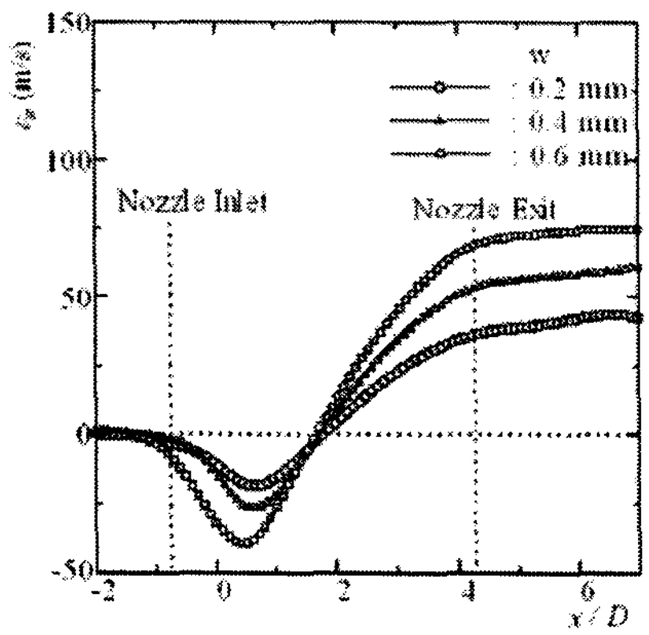

Fig.8. Axial velocity distributions on the centerline

the flow recirculation may have an important influence on the flow characteristics in the spiral flow nozzle.

Fig. 8 shows the axial velocity distributions on the centerline of nozzle with the slit width. As mentioned in Fig.7, the region of the flow recirculation is found for all cases and the velocity magnitude of the flow reversed is the highest in the slit width, w = 0.6mm and the lowest in w = 0.2mm. The position which its maximum value is found moves gradually to the nozzle upstream with the slit width. The position of stagnant point by the growth of boundary layer is almost same regardless of the slit width. However, axial velocity in the downstream of stagnant point is the highest in case of the slit width, w = 0.6mm. It is since the flow rate in the primary flow exhausted from annular slit is the highest in this case in comparison with other cases.

The tangential velocity distributions in radial direction in the nozzle are showing in Fig. 9. The tangential velocity distribution in the section A where axial velocity on the curve surface by Coanda effect is accelerated is decayed temporarily, but depending on the conservation of angular momentum in swirl tube, tangential velocity distributions in the nozzle increase gradually as goes to the downstream of nozzle with axial velocity. On the contrary, it can be expected that the radial velocity distributions in the nozzle decrease through the nozzle. The velocity distributions at a distance from nozzle exit are obtained. These results are showing in Fig. 10. In these results, axial and tangential velocities are non-dimensionalized to the maximum axial and tangential velocity obtained by the experiment. From these results, axial

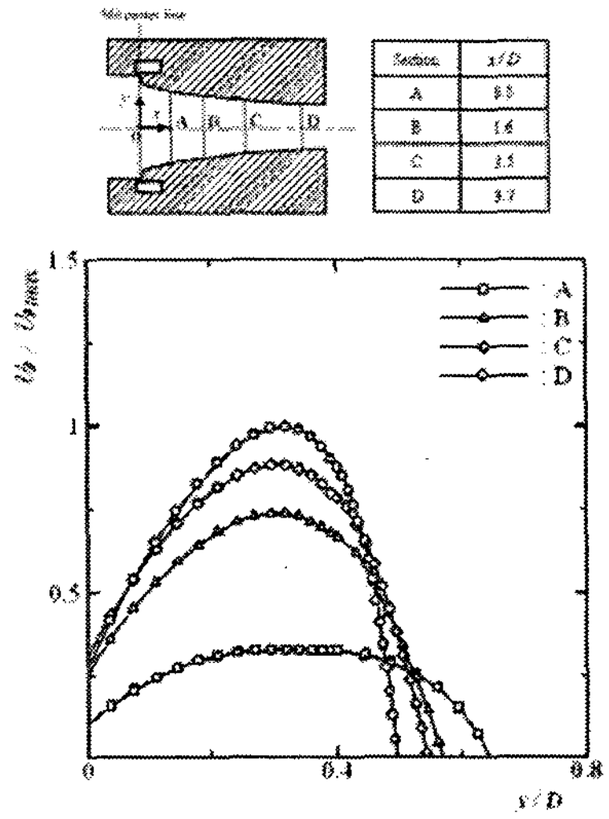

Fig.9. Tangential velocity distributions in radial direction

velocity obtained at a distance from nozzle exit increases with the slit width and for all cases, its velocity on the centerline of nozzle is lagged in comparison with that along the wall surface by the recirculation region generated around nozzle inlet by the growth of boundary layer between the primary flow and secondary flow induced from nozzle inlet. The tangential velocity also has the same trend as the axial velocity distribution.

However, depending on the tangential velocity

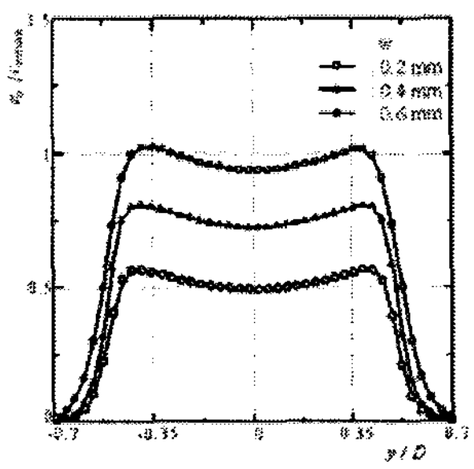

(a) Axial velocity distributions

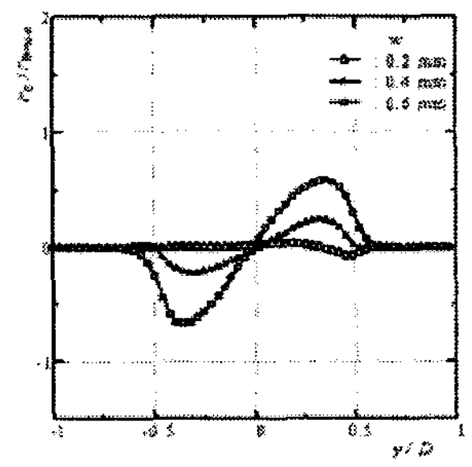

(b) Tangential velocity distributions

Fig. 10 Velocity distributions in radial velocity with the slit width (p_o / p_a = 1.28)

distributions detected at the tip of annular slit by the flow instability in the buffer, tangential velocity distributions in present position also have the highest value in the case of the slit width, w = 0.6mm and the lowest one in the case of w = 0.2mm. And its distributions in radial direction are not symmetric. As a result, the existence of tangential velocity at the tip of annular slit taken into account as the onset of spiral flow self-generated in the nozzle is deeply related with that of its velocity in the nozzle.

4. Conclusions

The self-generated mechanism of the spiral flow and the effect of nozzle configuration for the flow characteristics of spiral flow nozzle was clarified and investigated experimentally and numerically. The flow instability in the buffer region with time has an influence on the compressed air passing through annular slit. As a result, the tangential velocity distributions are found at the tip of annular slit. It can be considered as the onset of the spiral flow. The change of annular slit means that of the flow rate injected into nozzle from annular slit. Therefore, the axial velocity obtained at a distance from nozzle exit increase with the slit width and depending on the tangential velocity distributions obtained at the tip of annular slit, the tangential velocity is detected and also increases with the slit width.

References

[1] Bhagwat, M. J., Leishman, J G., "Correlation of Helicopter Rotor Tip Vortex Measurements", *AIAA Journal 38(2)*, (2000) pp. 301-308.

[2] Horii, K., Sawazaki, H., Matsumae, Y., Cheng, X. M., Take, M., Yasukawa, E. and Hashimoto, B., "New Continuous System for Dispersion and Encapsulation of Submicron Powders Using Spiral Flow", *ASME-Industrial Application of Fluid Mechanics*, Vol.FED-100, (1990), pp. 25-30.

[3] Horii, K., Matsumae, Y., Cheng, X. M., Takei, M. and Yasukawa, E., "Focusing Phenomena and Stability of Spiral-Flow Jet", *Trans. Japan Soc. Aero. Space Sci.*, **33**-102, (1991), pp. 141-153.

[4] Horii, K., Matsumae, Y., Ohsumi, K., Cheng, X. M., Kage, S. and Hashimoto, B., "Novel Optical Fiber Installation by Use of Spiral Flow", *J. of Fluids Engineering*, Vol. 114, (1992), pp. 373-378.

[5] Horii, K., Matsumae, Y., Cheng, X. M., Takei, M. and Hashimoto, B., "A Study of Spiral Flow (Part 4) The Effect of Radial Reynolds Number of Spiral Flow on Plasma Deposition of Pipe", *Trans. Japan Soc. Aero. Space Sci.*, **32**-98, (1992), pp. 165-175.

[6] Kreith, F. and Sonju, O. K., "The Decay of a Turbulent Swirl in a Pipe", *J. Fluid Mech.*, Vol.22, part2, (1965), pp.257-271.

[7] Miyazaki, K., Chen, G., Kudamatsuo, J., Sugimoto, T., Yamamoto, F. and Horii, K., "High-Efficiency Soil Transportation with Spiral Airflow", *Japan Soc. Aero. Space Sci.*, Vol. 42, No. 137, (1999), pp. 105-111.

[8] Spalart, P. R. and Allmaras, S. R., "A One-equation Turbulence Model for Aerodynamics Flows", *AIAA paper 92-0439*, (1992).

[9] Takei, M., Horii, K., Hashimoto, B., Kataoka, I., Ito, H. and Matsumae, Y., "High Stability of Spiral Jet – Relations between Axial Velocity Distribution and Stability", *J. of the Japan Soc. for Aeronautical and Space Sciences*, Vol. 43, No. 494, (1995), pp. 9-16.

[10] Takei, M., Horii, K., Hashimoto, B., Kataoka, I., Ito, H. and Matsumae, Y., "Cutting of Soft Materials Using of Spiral Water Jet", *J. of the Japan Soc. for Aeronautical and Space Sciences*, Vol. 42, No. 490, (1994), pp. 36-47.

[11] T. Nishizawa, K. Funatsu, K. Horii, and Y. Tomita, "Characteristics of turbulent swirling flow in a straight pipe", *Proceedings of JSME*, No.948-3, (1994), pp. 194-196.

[12] Ueda, H., Sakai, M., Horii, K., Funatsu, K. and Tomita, Y., "Study of Swirling Pneumatic Transport of Granule in a Horizontal Pipe", *Trans. Jpn. Soc. Mech.Eng.*, Vol. **67**, No. 664, (2001), pp. 3011-3017.

[13] Yamane, T, Yamamoto, K., Enomoto, S., Takaki, R., Tamazaki, H., Makida, M., Tamamoto, T., Iwamiya, T. and Nakamura, T., "Current Status of Common CFD Platform – UPACS", Proc. of Aerospace Numerical Simulation Symposium 2000, (2000), pp. 45-50.